Article:

Viehl, TP, Höffner, J, Lübken, F-J et al. (3 more authors) (2015) Summer time Fe depletion in the Antarctic mesopause region. Journal of Atmospheric and Solar-Terrestrial Physics, 127. 97 - 102. ISSN 1364-6826

https://doi.org/10.1016/j.jastp.2015.04.013

Summer time Fe depletion in the Antarctic mesopause region

T. P. Viehl[a], J. Höffner[a], F.-J. Lübken[a], J.M.C. Plane[b], B. Kaifler[a,c], R.J. Morris[d]

[a] *Leibniz-Institute of Atmospheric Physics (IAP) at the University of Rostock, Schloßstr. 6, 18225 Kühlungsborn, Germany*
[b] *School of Chemistry, University of Leeds, Leeds LS2 9JT, United Kingdom*
[c] *German Aerospace Centre (DLR), Institute of Physics of the Atmosphere, Münchner Str. 20, 82234 Wessling, Germany*
[d] *Australian Antarctic Division (AAD), 203 Channel Hwy, Kingston, Tasmania 7050, Australia*

Abstract

We report common volume measurements of Fe densities, temperatures and ice particle occurrence in the mesopause region at Davis Station, Antarctica (69°S) in the years 2011–2012. Our observations show a strong correlation of the Fe-layer summer time depletion with temperature, but no clear causal relation with the onset or occurrence of ice particles measured as noctilucent clouds (NLC) or polar mesosphere summer echoes (PMSE). The combination of these measurements indicates that the strong summer depletion can be explained by gas-phase chemistry alone and does not require heterogeneous removal of Fe and its compounds on ice particles.

Keywords: Mesospheric iron, Noctilucent clouds, Polar mesospheric clouds, Polar mesosphere summer echoes, Heterogenous chemistry

PACS: 92.60.Hc, 92.60.Mt, 93.30.Ca, 93.30.Sq, 93.85.Pq

Email address: `viehl@iap-kborn.de` (T. P. Viehl)

1. Introduction

When meteors enter the Earth's atmosphere they predominantly ablate in an altitude region between 75 and 115 km. Ablated meteoric metal atoms form layers of neutral, ionised and molecular bound species, the latter mainly in the form of oxides and hydroxides (*Self and Plane*, 2003). The seasonal change in metal abundance is largely determined by the seasonal variation in global circulation and temperature dependent chemistry (*Plane et al.*, 2015). In a recent study *Feng et al.* (2013) compare the seasonal variation at several sites (including measurements at Davis, Antarctica) with model calculations and list comprehensive references.

Another phenomenon characteristic to the MLT altitude range is the summer time occurrence of ice particles at polar latitudes. These ice particles can be detected by satellites, lidar instruments or the human eye when they have reached sufficient size (with radii typically larger than 20 nm) through condensation growth. In the case of satellite observations the ice particles are known as polar mesospheric clouds (PMC), in the case of ground based observations as noctilucent clouds (NLC), e.g. (*Baumgarten et al.*, 2012; *DeLand et al.*, 2006; *Russell et al.*, 2009; *Lübken et al.*, 2009). Visibly observable ice particles as well as smaller, sub-visible ice particles can lead to polar mesosphere summer echoes (PMSE), which are strong radar echoes caused by small scale structures in electron densities (*Rapp and Lübken*, 2004). These structures on the order of the radar Bragg wavelength rely on the combined effect of neutral air turbulence and charged ice particles. It is important to note that PMC and NLC require 'large' ice particles whereas PMSE can also be caused by smaller ice particles ($r \leq 20$ nm). Consequently, PMC/NLC appear at the lower edge of the super-saturated region (approximately 82–84 km) whereas PMSE extend to higher altitudes (up to 94 km).

Observations by *Plane et al.* (2004); *Lübken and Höffner* (2004) and subsequent studies investigated the uptake of metal atoms, in particular of Fe (iron) and K (potassium), on ice particles. These authors report singular events of metal atom depletions with simultaneous occurrence of PMSE as well as NLC in the case of K, and NLC in the case of Fe. *She et al.* (2006) and *Thayer and Pan* (2006) found similar anti-correlations for Na (sodium). These studies suggest that the depletion is largely caused by an uptake of metal atoms on the ice particle surface. For K, this was reproduced in a model by *Raizada et al.* (2007). Northern hemispheric K densities were shown to fall nearly instantaneously at the beginning of the PMSE and NLC season. K densities remained low and steady for the period of ice particle occurrence. Similarly to the beginning of the season, densities increased markedly at the end of the PMSE season, i.e. when no further ice particles were observed.

The hypothesis of metal atom adsorption on ice particles was developed further to explain the summer time behaviour of the seasonal Fe cycle in the MLT region of the Southern Hemisphere. *Gardner et al.* (2011) compared observations performed at Rothera, Antarctica (*Chu et al.*, 2006) and the South Pole (*Gardner et al.*, 2005). Both Rothera and the South Pole show significant Fe depletion at around 80–92 km during the summer months and in particular during a period of about ± 40 days around summer solstice when NLC are observed. Differences in metal layer abundance, height and width between these two stations were attributed to differences in NLC altitude, brightness and occurrence frequency. Spatial and temporal mismatches between the presence of NLC particles and Fe depletion were noted, observable mostly above 87 km altitude and in the month prior to the first NLC detection. Common volume comparisons of Fe densities with PMSE were so far not available. In analogy to results from other metals in the Northern Hemisphere and due to promising modelling efforts, these gaps were attributed to smaller, sub-visible particles.

Gardner et al. (2011) found a high positive correlation of Fe densities with temperature as expected from calculations by *Plane* (2003) and others and discuss various influences on the seasonal variation of the metal layer. The authors concluded that the peak of the Fe layer was pushed to well above 90 km because persistent ice clouds at lower altitudes removed the Fe atoms in vicinity.

Hence, according to all those studies cited above it seems that the summer time Fe depletion in the Antarctic mesopause region is largely influenced by the uptake of metal atoms on ice particles. We present observations which challenge this hypothesis.

2. Instrumentation

The mobile Fe-Lidar operated by the Leibniz-Institute of Atmospheric Physics (IAP) was commissioned at Davis, Antarctica (68.6°S, 78.0°E) in the early summer season 2010–11 (*Lübken et al.*, 2011; *Morris et al.*, 2012). It was in operation for more than two consecutive years until the end of the summer season 2012–13 in early January 2013. The lidar is a two-wavelength system based on a frequency-doubled alexandrite laser (*von Zahn and Höffner*, 1996; *Höffner and Lautenbach*, 2009). It is capable of determining mesospheric temperatures and Fe densities in full daylight by scanning the Doppler broadened Fe resonance line at 386 nm. High solar background as well as low Fe densities are the conditions giving the largest possible measurement uncertainty. Typical uncertainties for temperatures are 5 K for 1 hour integration and 1 km altitude range in summer time during noon conditions and annual low Fe density. Uncertainties for daily means are on the order of 1 K and less than 1 % for temperature and Fe density, respectively. Variations in uncertainties depend on tropospheric weather, absolute Fe densities and observation period. NLC are simultaneously detected by an independent analysis of the retrieved residual infrared laser wavelength at 772 nm. As the system is capable of nearly background free single photon detection during full daylight, NLC are detectable within an integration time as short as 2 minutes. The complete dataset obtained by the mobile Fe-Lidar at Davis includes 2900 hours of lidar measurements nearly equally distributed throughout the year and all hours of the day. During the austral summer months September 2011 to March 2012 a total of 1151 hours of temperature and density measurements with at least 1 hour duration were obtained on 94 days. The average length of the measurements considered is 12 hours 14 minutes per day.

Another instrument operated at Davis is the 55 MHz Mesosphere-Stratosphere-Troposphere (MST) radar of the Australian Antarctic Division (AAD) which was put into operation in the summer season of 2002–03 (*Morris et al.*, 2004). This system has been detecting PMSE on a regular basis since the summer season 2003–04. The AAD MST radar was in operation during all times when the IAP Fe-Lidar was in operation. As both instruments are located at Davis, common volume measurements of Fe densities, temperatures and ice particles (detected as NLC and PMSE) are available and allow a unique combined analysis of these atmospheric features.

3. Observations of Fe density, temperature and ice particles

3.1. Fe density and temperature in the 2011/12 summer

Fig. 1 shows Fe densities and temperatures in the mesopause region from spring to autumn. Fe densities are cut off at $100\,\mathrm{cm}^{-3}$. In general, densities and temperatures during the summer months are at their annual low with daily mean temperatures between 87 and 95 km lower than 145 K and densities lower than $10{,}000\,\mathrm{cm}^{-3}$ except for higher densities in the peak layer from mid-February onwards. Contrary to model results (*Feng et al.*, 2013) and previous observations (*Gardner et al.*, 2011) for this Antarctic latitude, the upper boundary of the Fe layer at Davis as shown in Fig. 1 is generally higher during the summer months than during spring and autumn. (See, e.g., the $2{,}000\,\mathrm{cm}^{-3}$ contour line.) High densities at high altitudes in late March are caused by sporadic layers. The centroid altitude rises towards summer solstice and falls thereafter, as the whole Fe layer is shifted upwards. The whole layer thins out throughout all altitudes towards solstice. The figure also shows a very strong short term depletion in Fe densities of about 2 weeks duration around solstice between 87 and 95 km altitude. Simultaneously, record low daily average temperatures below 135 K are shown in the exact same altitude and time region. Some of these temperatures as well as singular short term profiles have recently been published by *Lübken et al.* (2014). Fig. 1 therein shows temperatures as low as 100 K on 17/18

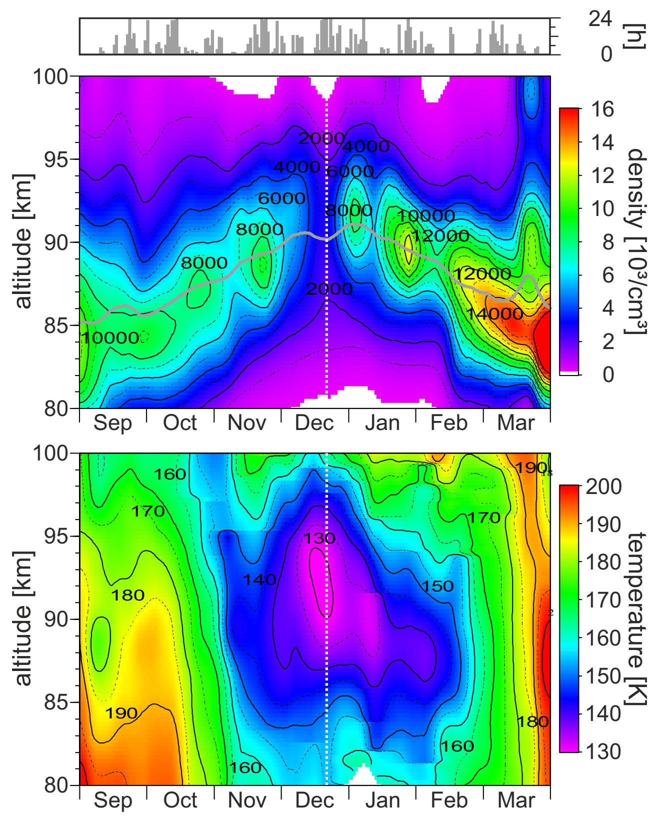

Figure 1: Fe densities (upper panel) and temperatures (lower panel) September 2011 to March 2012. Lidar measurement periods are displayed as histogram for 0–24 hrs per day on the very top. The Fe layer's upper boundary and centroid altitude (grey line) are elevated around summer solstice (white dotted line). Very low densities around solstice coincide with very low temperatures.

December 2011.

3.2. Fe density and ice particles

It is well known that low temperatures lead to ice nucleation and successively to the creation of PMSE (*Rapp et al.*, 2002). Simultaneously, it has been shown that low temperatures alter the chemical reactions in the MLT region such that the amount of free, neutral Fe atoms is reduced (*Feng et al.*, 2013). When investigating the causal relationship of ice particle occurrence and the summer time Fe depletion in the Antarctic mesopause region, an obvious problem is therefore to separate those effects. Are low temperatures causing ice particles and are those ice particles then significantly reducing available Fe atoms? Or are low temperatures on their own altering the chemical equilibrium so profoundly that Fe atoms are efficiently converted to reservoir species and disappear—even without adsorption on ice particles in the vicinity? Do we observe a combination of both effects?

To answer these questions we have analysed the annual cycle of the Fe column densities rather than studied a time-altitude plot as in Fig. 1. We see justification for the investigation of column densities in the fact that these should generally decrease in the presence of ice particles at any altitude within the metal layer provided that the seasonal variations of other effects such as the meteor input function (*Feng et al.*, 2013) are comparatively small in that period. As was shown in the case of K in model calculations by *Raizada et al.* (2007), a potential localised removal of metal atoms at any given altitude will affect the whole layer due to vertical eddy diffusion. Setting aside all other effects such as transport and meteoric input, column densities should be generally lower whenever ice particles are present and remove metal atoms

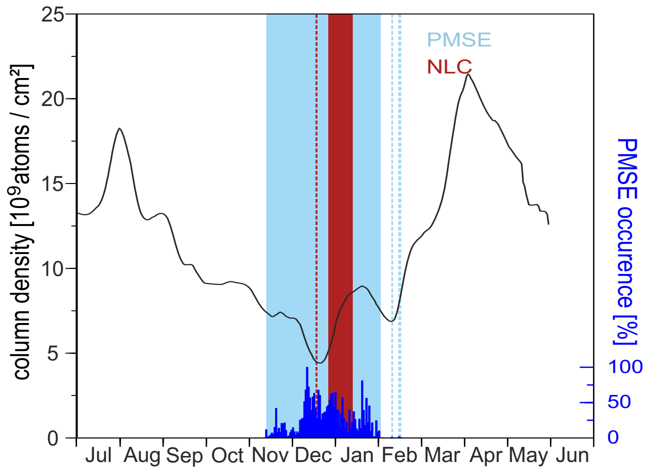

Figure 2: Annual cycle of column densities of Fe from July 2011 to May 2012. Ice particle measurements are highlighted in blue and red (PMSE and NLC, respectively). The blue histogram shows the occurrence statistics for PMSE. Dashed lines indicate singular, weak PMSE and NLC events outside the main occurrence periods. Note the decline in Fe densities before the onset of ice particle occurrence and the increase during the main NLC period.

significantly. Furthermore, if ice particles have a significant effect on the seasonal metal layer, then column densities should be expected to show a non-steady behaviour with the onset and suspension of ice particle occurrence.

Fig. 2 shows Fe column densities between July 2011 and May 2012. Column densities are calculated as the integrated densities of the whole MLT neutral Fe layer from the lower edge at about 75 km altitude to 120 km. In general, more than 99 % of the Fe atoms are confined to the layer between its lower edge and about 105 km. Only minor amounts of metal atoms are found above this altitude in the daily and annual mean. Model studies have investigated the general behaviour of the Fe-layer at polar latitudes (e.g., *Feng et al.*, 2013). In accordance with these results, winter column densities at Davis are typically larger than $10 \times 10^9\,\mathrm{cm}^{-2}$. Our measurements show a steady decline in column densities from early August to late November.

The summer state of the atmosphere at Davis from mid-November to early February is characterised by relatively low MLT Fe column densities of about 6–8$\times 10^9\,\mathrm{cm}^{-2}$. For a short period around solstice, column densities drop below $5 \times 10^9\,\mathrm{cm}^{-2}$. The average peak density at summer solstice observed during a measurement period lasting 15.9 hours on 20/21 December 2011 is only 1,000 cm^{-3} between 90–93 km. This feature lasts for only a few days and is thus partly smoothed out by the 2-week Hanning window applied to the Fe density dataset used in Fig. 2. The autumn increase in densities begins towards the end of December, with a particularly interesting local maximum in Fe densities with over $8 \times 10^9\,\mathrm{cm}^{-2}$ in late January.

Also shown in Fig. 2 is the occurrence of larger ice particles (NLC) from mid-December to mid-January. The red shaded area marks the period between 27 December 2011 and 12 January 2012 when nearly all of the NLC were observed. During this main NLC period 94 hours of lidar observations were obtained on 9 days. NLC occurred over 42.5 % of the time. The red dashed line marks a very weak and short singular NLC event on 17 December 2011 prior to the main NLC period, which is only visible after unusually long integration of more than 20 minutes. No NLC were observed at any other time during the observations. In particular, no NLC were observed when Fe column densities were at a seasonal low, namely between 17 December and 26 December—even though 130 hours of observation were obtained during these 9 days. Additionally, PMSE are shown in Fig. 2. While average temperatures are still decreasing around mid-November, the onset of the first sporadically developing PMSE is dominated by cold phases of waves (predominantly gravity waves) which are capable of enhancing or destroying ice particles (*Rapp et al.*, 2002). PMSE occurrence is therefore low in the period 17–24 November 2011, with PMSE only observable 6.2% of the time (see histogram in Fig. 2). When average temperatures have dropped to the annual summer low in mid-December, PMSE appear every day. Average occurrence per day is 77.2% in the week around solstice with a maximum of 94.1%.

3.3. Temperature dependence

Fig. 1 displays a striking overlap of very low temperatures and low Fe densities in mid-December. We use this prominent time and altitude frame to investigate the relationship between temperatures and Fe densities in more detail. Fig. 3 illustrates the relationship between the Fe density and average temperature between 87 and 92 km, over a ± 40 day window around solstice in the summer months 2011–2012. Included in these calculations are 39 daily mean temperatures and Fe densities from all measurements with more than 6 hrs duration, totalling 591 hrs of measurements.The data is plotted in the Arrhenius form, yielding an activation energy of $11.2 \pm 1.5\,\mathrm{kJ\,mol^{-1}}$.

Table 1 lists the important reactions which convert iron between atomic Fe and its main reservoir, FeOH (*Plane et al.*, 2015). Formation of FeOH starts with R1 which produces FeO. There is then competition between R2 and R3, with the latter further oxidizing FeO to FeO_2 (R4 is pressure-dependent and too slow above 82 km to compete with R3). FeO_2 is then oxidized by O_3 to make FeO_3, which is eventually converted to the reservoir FeOH either directly via R11 or indirectly via R8 followed by R10. Inspection of the rate coefficients shows that once Fe has been oxidized to FeO_2,

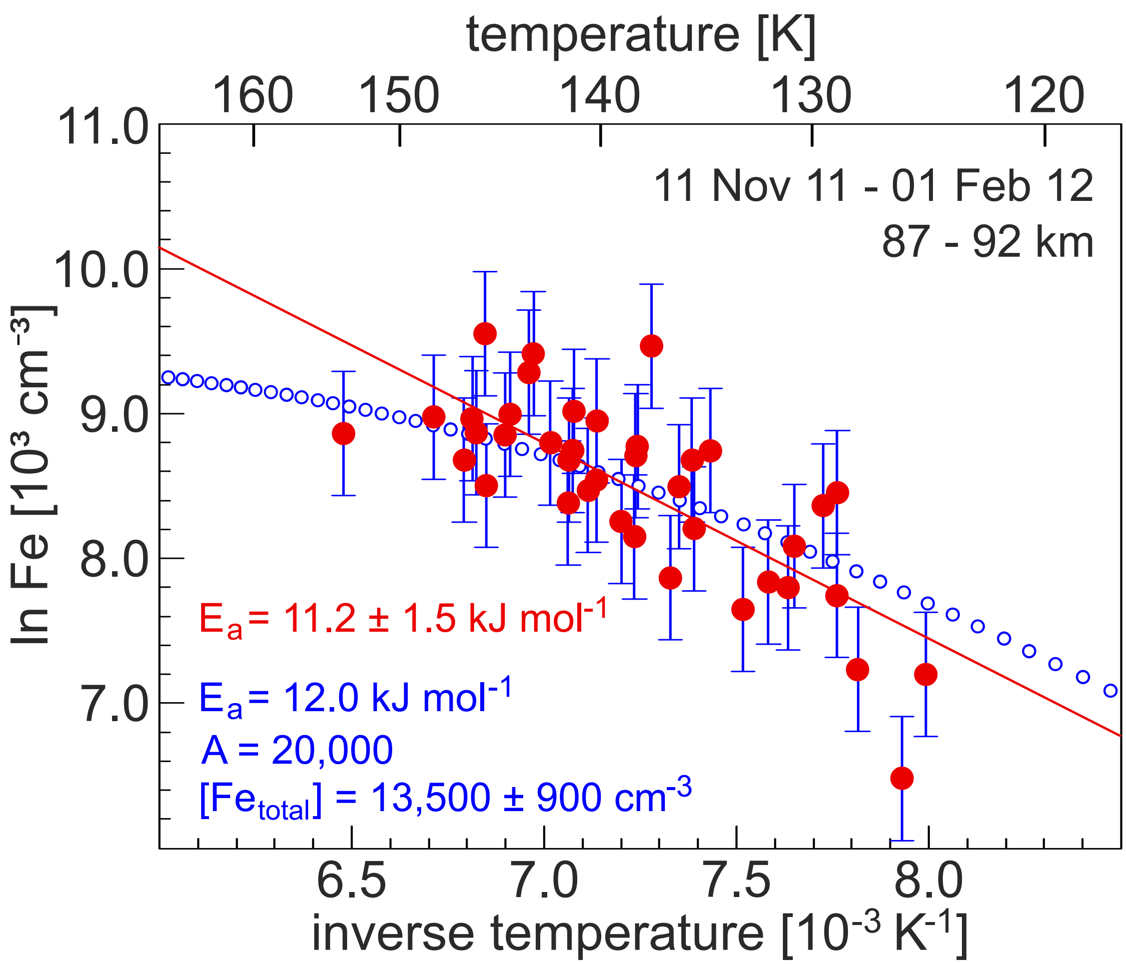

Figure 3: Arrhenius plot for the potential chemical reactions dominating the strong depletion of atomic Fe between 87 and 92 km, between 11.11.2011 and 01.02.2012. The activation energy calculated from the slope of a linear regression is $11.2 \pm 1.5\,\mathrm{kJ\,mol^{-1}}$. A good fit to the data is achieved for $E_a = 12.0\,\mathrm{kJ\,mol^{-1}}$, $A = 2 \times 10^4$ and a total Fe abundance of $[\mathrm{Fe_{total}}] \approx [\mathrm{Fe}] + [\mathrm{FeOH}] = 13,500\,\mathrm{cm^{-3}}$. See text for details.

conversion to FeOH is much more likely than reduction by atomic O, since the activation energies of R5 and R7 are comparatively large.

Yu et al. (2012) have presented an analysis of the solar influence on the altitude of the Fe layer bottomside. This effect is caused by the photolysis R13: FeOH + h$\nu \longrightarrow$ Fe + OH and regularly observed at Davis whenever the solar elevation passes $-5°$, i.e. the altitude of the mesopause changes from being either sunlit or not. The rapid appearance of Fe below 80 km at sunrise is consistent with the photolysis rate of FeOH being much faster than the rate adopted in *Feng et al.* (2013). Recent analysis of data from Davis indicates that J_{13}(FeOH) is around $2 \times 10^{-3}\,\mathrm{s}^{-1}$ (*Viehl, Feng and Plane* (2015), *personal communication*). Taking all this into account, the rate of change of the Fe concentration, $d[Fe]/dt$,may be written as the sum of loss and production terms, which is approximately equal to zero at steady state:

$$\frac{d[\mathrm{Fe}]}{dt} = -k_1[\mathrm{Fe}][\mathrm{O_3}]\left(\frac{k_3[\mathrm{O_3}]}{k_2[\mathrm{O}] + k_3[\mathrm{O_3}]}\right) + (k_{12}[\mathrm{H}] + J_{13})[\mathrm{FeOH}] \approx 0$$

Since $k_2[\mathrm{O}] \gg k_3[\mathrm{O_3}]$ and also $J_{13} \gg k_{12}[\mathrm{H}]$,

$$-k_1[\mathrm{Fe}][\mathrm{O_3}]\frac{k_3[\mathrm{O_3}]}{k_2[\mathrm{O}]} + J_{13}[\mathrm{FeOH}] \approx 0$$

The partitioning of iron between Fe and FeOH is therefore given by the ratio χ:

$$\chi = \frac{[\mathrm{Fe}]}{[\mathrm{FeOH}]} = \frac{J_{13}k_2[\mathrm{O}]}{k_1k_3[\mathrm{O_3}]^2}$$

The O_3 concentration in the MLT is approximately in steady state between formation and loss by photolysis and the reaction with H:

$$\mathrm{O} + \mathrm{O_2}(+\mathrm{M}) \longrightarrow \mathrm{O_3} \qquad k_{14} = 2.5 \times 10^{-34} \exp(380/T) \mathrm{cm^6\,s^{-1}}$$

$$\mathrm{O_3} + \mathrm{h}\nu \longrightarrow \mathrm{O} + \mathrm{O_2} \qquad J_{15} = 8 \times 10^{-3}\,\mathrm{s^{-1}}$$

$$\mathrm{O_3} + \mathrm{H} \longrightarrow \mathrm{OH} + \mathrm{O_2} \qquad k_{16} = 1.4 \times 10^{-10} \exp(-470/T) \mathrm{cm^3\,s^{-1}}$$

so $[\mathrm{O_3}] = k_{14}[\mathrm{O}][\mathrm{O_2}][\mathrm{M}]/(J_{15} + k_{16}[\mathrm{H}])$. As the solar elevation at Davis is larger than $-5°$ within ± 40 days of the summer solstice, the MLT region is constantly sunlit. Therefore, since $J_{15} > k_{16}[\mathrm{H}]$, $[\mathrm{O_3}] \approx k_{14}[\mathrm{O}][\mathrm{O_2}][\mathrm{M}]/J_{15}$ and χ can be expressed as

$$\chi = \frac{[\mathrm{Fe}]}{[\mathrm{FeOH}]} = \frac{J_{13} k_2 [\mathrm{O}] J_{15}^2}{k_1 k_3 (k_{14}[\mathrm{O}][\mathrm{O_2}][\mathrm{M}])^2}$$

[O] is not strongly temperature-dependent but largely governed by photochemistry. Since the data is taken over a constant altitude range of less than a scale height, the pressure is nearly constant. [O], $[\mathrm{O_2}]$ and [M] will therefore vary as T^{-1} around the geometric mean temperature in this altitude and time range, $T_{\mathrm{eff}} = 136\,\mathrm{K}$. Hence, expressing χ in the Arrhenius form $\chi = A \exp(-E/T)$, the activation energy E is given by

$$E = -E_1 - E_3 + E_2 - 2 \times E_{14} + 5 \times T_{\mathrm{eff}}$$

where E_i corresponds to the activation energy of reaction i divided by $R = 8.314\,\mathrm{J\,K^{-1}\,mol^{-1}}$ as taken from *Plane et al.* (2015). E is thus $(-174 - 177 + 350 + 2 \times 380 + 5 \times 136) = 1439\,\mathrm{K}$, or about $12.0\,\mathrm{kJ\,mol^{-1}}$.

The total amount of Fe, $[\mathrm{Fe_{total}}] \approx [\mathrm{Fe}] + [\mathrm{FeOH}]$, should be approximately constant during this mid-summer period, since $[\mathrm{Fe_{total}}]$ is a function of the meteoric injection rate and transport. Thus,

$$[\mathrm{Fe}] = \frac{\chi}{1+\chi}[\mathrm{Fe_{total}}]$$

The data (red daily means) in Fig. 3 can then be fitted with three parameters, E_a, A and [Fe_{total}]. The pre-exponential factor A is given by

$$A = \frac{J_{13} A_2 [\mathrm{O}] J_{15}^2}{A_1 A_3 (A_{14} [\mathrm{O}][\mathrm{O_2}][\mathrm{M}])^2}$$

where A_i refers to the pre-exponential factor of reaction i in Table 1. Taking $[\mathrm{O}] = 6 \times 10^{11}\,\mathrm{cm}^{-3}$, $[\mathrm{O_2}] = 1.3 \times 10^{13}\,\mathrm{cm}^{-3}$, and $[\mathrm{M}] = 6.4 \times 10^{13}\,\mathrm{cm}^{-3}$ at 90 km and $T = 135\,\mathrm{K}$ (*Plane et al.*, 2015), A can be estimated as 2×10^4. A very satisfactory fit (blue circles in Fig. 3) is achieved with $E_a = 12.0\,\mathrm{kJ\,mol}^{-1}$, $A = 2 \times 10^4$ and $[\mathrm{Fe_{total}}] = 13,500 \pm 900\,\mathrm{cm}^{-3}$. The blue errorbars are calculated as RMS of the daily means to the fit.

Since not all activation energies listed in Table 1 are well known and several simplifying assumptions have been made in the above calculation, an additional role played by the uptake of Fe and FeOH on ice particles at low temperatures cannot be ruled out. However, this exercise demonstrates that the decrease of Fe between 87 and 92 km which is observed in mid-summer can be explained by gas-phase chemistry alone.

4. Discussion

Due to the unique combination of radar and lidar instruments at Davis, we are able to directly investigate the correlation between large and small ice particles (NLC and PMSE) and Fe densities. A striking feature of Fig. 2 is the onset of the Fe depletion before the first occurrence of NLC and PMSE. Furthermore, not only are column densities dropping before a maximum in NLC brightness and occurrence frequency is observed in early January, they even increase significantly during the main NLC period. Indeed, a local

Number	Reaction	Rate Coefficient
R1	$Fe + O_3 \longrightarrow FeO + O_2$	$2.9 \times 10^{-10} \exp(-174/T)$
R2	$FeO + O \longrightarrow Fe + O_2$	$4.6 \times 10^{-10} \exp(-350/T)$
R3	$FeO + O_3 \longrightarrow FeO_2 + O_2$	$3.0 \times 10^{-10}(-177/T)$
R4	$FeO + O_2(+M) \longrightarrow FeO_3$	$4.4 \times 10^{-30} \exp(T/200)^{0.606}$
R5	$FeO_2 + O \longrightarrow FeO + O_2$	$1.4 \times 10^{-10} \exp(-580/T)$
R6	$FeO_2 + O_3 \longrightarrow FeO_3 + O_2$	$4.4 \times 10^{-10} \exp(-170/T)$
R7	$FeO_3 + O \longrightarrow FeO_2 + O_2$	$2.3 \times 10^{-10} \exp(-2310/T)$
R8	$FeO_3 + H_2O \longrightarrow Fe(OH)_2 + O_2$	5×10^{-12}
R9	$FeO + H_2O(+M) \longrightarrow Fe(OH)_2$	$5.1 \times 10^{-28} \exp(-200/T)^{1.13}$
R10	$Fe(OH)_2 + H \longrightarrow FeOH + H_2O$	$3.3 \times 10^{-10} \exp(-302/T)$
R11	$FeO_3 + H \longrightarrow FeOH + O_2$	$3.0 \times 10^{-10} \exp(-796/T)$
R12	$FeOH + H \longrightarrow Fe + H_2O$	$3.1 \times 10^{-10} \exp(-1264/T)$
R13	$FeOH + h\nu \longrightarrow Fe + OH$	2×10^{-3}

Table 1: Reactions of neutral Fe-containing species in the MLT. R1 to R12 taken from (Plane et al., 2015). M in R4 and R9: N_2 and O_2. Units of rate coefficents: k_i bimolecular, $cm^3\,molecule^{-1}\,s^{-1}$; k_i termolecular, $cm^6\,molecule^{-2}\,s^{-1}$, J_i: s^{-1}

column density maximum of $\sim 8 \times 10^9\,\mathrm{cm}^{-2}$ occurs in mid-January when NLC and PMSE occurrence is high. Densities in this period are nearly as high as in mid-September, i.e. well before the summer transition of the MLT. Moreover, no sharp drop in column density, layer shape or other parameters are observed with the beginning and end of both the PMSE and NLC season, in contrast to K observations in the Northern Hemisphere. This is strong evidence that an uptake of Fe on ice particles cannot be the major driving factor in the change of the annual cycle of Fe densities leading to the strong summer time depletion. The density drop is taking place considerably earlier than ice particles occur and shows an unexpected anti-correlated behaviour in January.

These observations question explanations of differences in the midsummer Fe layer behaviour between two Antarctic stations published previously (*Gardner et al.*, 2011). That study attributed the annual change—and especially the summer time Fe depletion below 95 km altitude—to the uptake of Fe on NLC particles. A one-to-one comparison between that work and the current study is not straightforward, as the dataset presented in the earlier study is not only at a different longitude, but includes considerably fewer hours and days of measurement. This was perhaps one reason that those authors applied an harmonic fit to the data. A detailed comparison of the harmonically fitted data with the higher resolution dataset (smoothed with a 14 day Hanning window) presented here may yield misleading results based on the different mathematical treatment of the data, and not on geophysics. For example, the raw data in Fig. 1 in *Gardner et al.* (2011) shows an indication of low densities for two weeks in mid-December and higher densities in January at Rothera. This feature however disappears after applying the harmonic fit, as a comparison with Fig. 2 therein shows. We conclude from the available datasets that Fe depletion and NLC occurrence are both caused by low temperatures, and not necessarily one by the other.

However, we note that this does not contradict a localised metal uptake by NLC particles as presented by *Plane et al.* (2004). Those authors observed almost complete removal of Fe within very strong NLCs with high volumetric surface areas. Such localised "bite-outs" (in a vertical sense) are not explicable by gas-phase chemistry, and occur because heterogeneous removal is fast enough to compete with vertical mixing and fresh meteoric ablation. However, heterogeneous removal within weaker NLCs will be difficult to discern from gas-phase removal. As ice particles in the MLT have a relatively short life time compared to the seasonal change, a local uptake might be not large enough or last long enough to significantly impact the entire Fe layer on a seasonal scale.

Murray and Plane (2005) investigated the uptake coefficients for various metals. That study found uptake coefficients for K and Na on cubic ice close to unity. For Fe, an uptake coefficient close to unity was found for higher temperatures above 140 K as well, but this decreased rapidly for temperatures lower than 135 K to $\gamma_{\mathrm{Fe}} = 3 \times 10^{-3}$ at 80 K. A lower relative importance of metal uptake on ice particles for Fe at Antarctic sites compared to neutral gas chemistry might therefore be caused by the very low mesopause temperatures of down to 100 K in waves and less than 135 K in the daily mean around summer solstice.

We conclude that ice particles in general (NLC and PMSE) and low Fe densities at Antarctic sites largely occur simultaneously during the summer period since they are both consequences of low temperatures. An uptake of Fe atoms on ice particle surfaces cannot be excluded, but is not the driving factor in the annual change of Fe density.

This interpretation is supported by WACCM-Fe calculations which show a strong positive correlation between Fe density and temperature and a decrease in column abundance as observed at Davis, Rothera and the South Pole. Although Fe density is further reduced if an uptake on ice particles is considered, the model captures the seasonal variation of Fe even without PMC scheme (*W. Feng* (2015), *personal communication*). The model simulations yield realistic results but are limited by the underlying temperature field and circulation used in WACCM. In particular, the high summer mesopause altitude and extremely low mesopause temperatures reported by *Morris et al.* (2012) and *Lübken et al.* (2014) have not yet been reproduced. Additionally, absolute density calculations crucially rely on a realistic representation of the meteoric influx as well as careful balancing of reaction rate coefficients. The magnitude of the meteoric influx is a matter of ongoing discussion (*Plane*, 2012) and not all reactions rates are so far well known from laboratory experiments. Further WACCM-Fe results with improved rate coefficients and better temperature representation might give even better insights in the behaviour of the metal layer.

We want to further point to the uplift of the Fe layer's centroid altitude in the upper panel of Fig. 1. We emphasise that the whole layer including the upper boundary is shifted upwards and that the lower boundary is nearly linearly shifted upwards from September onwards, clearly before the onset of ice particles. This is not simply a relative shift due to a depletion in the lower parts of the MLT Fe layer. We interpret the summer time uplift of the centroid altitude, previously also reported by *Gardner et al.* (2005, 2011) and others, to be caused by the summer time dynamic uplift at polar latitudes. Other possible causes could be the changed chemical equilibrium between Fe and its reservoir species due to drastically changed temperatures and solar irradiance. However, it should be noted that increased conversion of Fe to Fe^+ on the topside of the layer—caused by charge transfer with NO^+ and ${O_2}^+$ ions and photo-ionisation—should depress the topside of the Fe layer. This makes the uplift all the more striking.

The calculations presented in section 3.3 confirm that temperature dependent chemical reactions play a significant role in the annual cycle of Fe. They alter the equilibrium between atomic Fe and its molecular bound species in such a way that low temperatures favour the latter over the former and remove Fe. These considerations on their own do not completely rule out an additional metal uptake on ice particles. However, the calculations show that under reasonable assumptions neutral gas chemistry alone can explain the strong summer time Fe depletion in the Antarctic mesospause region. Further comprehensive 3D model calculations as performed by WACCM-Fe, laboratory studies of metal containing species and analyses of atmospheric measurements are necessary to improve our knowledge about important reaction rate coefficients. This will help to determine the exact contribution of all chemical reactions, transport and a potential additional effect of ice particle adsorption on the mesospheric Fe layer.

At this point, we cannot provide measurements of winds to analyse the role of latitudinal transport. Future simulations such as performed by *Feng et al.* (2013) might help to understand the relative importance of horizontal or vertical transport in relation to the chemical analysis performed here. The role of wintertime convergence and summertime divergence over the South Pole was first proposed by *Gardner et al.* (2005) to explain the very large seasonal variation of Na and Fe observed. However, the importance of horizontal transport depends on the residence time of Fe and its reservoirs above 80 km, and hence to the rate of vertical transport. More understanding of these processes is required.

Note that optical measurements at polar latitudes pose a significant technological challenge around summer solstice. The mid-December features presented here require regular measurements in a period of a few weeks. In particular the brief low temperatures coinciding with low absolute Fe densities might be easily missed by instruments with low SNR.

5. Conclusion

Our calculations show that neutral gas-phase chemistry alone can explain most of the strong summer time Fe depletion in the Antarctic mesopause region. The measurements presented here show that ice particle occurrence does not appear to be the dominant driving factor in the summer time depletion of the annual cycle of the Fe layer in the mesopause region at Davis, Antarctica. Although conclusive evidence for the uptake of various metals on ice particles has been reported for singular measurements by several authors, the effect alone cannot explain the seasonal Fe layer cycle presented in this study.

Our measurements show a general uplift of the Fe layer during the summer months including the upper boundary. An increase of the layer's centroid altitude due to heterogenous removal of Fe and FeOH on on the underside of the layer alone is therefore not sufficient to account for this.

A detailed analysis of the intraday variability in Fe density, the correlation with temperature and the occurrence of ice particles such as NLC and PMSE on short time scales will be the subject of further studies. This will help to quantify the uptake rates of Fe atoms on ice particles and thus help to understand how large or small an additional uptake effect is on short time scales and at various temperature regimes. A further combination of chemical modelling with the input of our observational data will help to gain a better understanding of the chemical processes involved.

Acknowledgement

This project was funded by the Australian Antarctic Division under AAP 2325 and the Leibniz-Institute of Atmospheric Physics. J. M. C. Plane's work is supported by the European Research Council (project number 291332-CODITA). We thank W. Feng, G. Sonnemann and J. C. Gómez Martín for fruitful discussions about Fe chemistry as well as A. D. James for helpful comments on the paper. We thank R. Latteck for his help in preparing PMSE data.

We would like to express our special gratitude to all expeditioners of the 64$^{\mathrm{th}}$, 65$^{\mathrm{th}}$ and 66$^{\mathrm{th}}$ ANARE at Davis Station for their dedicated support throughout the project.

References

Baumgarten, G., A. Chandran, J. Fiedler, P. Hoffman, N. Kaifler, J. Lumpe, A. Merkel, C. E. Randall, D. Rusch, and G. Thomas (2012), On the horizontal and temporal structure of noctilucent clouds as observed by satellite and lidar at ALOMAR (69N), *Geophys. Res. Lett.*, *39*, L01803, doi: 10.1029/2011GL049935.

Chu, X., P. J. Espy, G. J. Nott, J. C. Diettrich, and C. S. Gardner (2006), Polar mesospheric clouds observed by an iron Boltzmann lidar at Rothera (67.5°S, 68.0°W), Antarctica, from 2002 to 2005: Properties and implications, *J. Geophys. Res.*, *108*, doi:10.1029/2002JD002524.

DeLand, M. T., E. P. Shettle, G. E. Thomas and J. J. Olivero (2006), A quarter-century of satellite polar mesospheric cloud observations, *J. Atmos. Solar-Terr. Phys.*, *68*, 9–29, doi:10.1016/j.jastp.2005.08.003

Feng, W., D. R. Marsh, M. P. Chipperfield, D. Janches, J. Höffner, F. Yi, and J. M. C. Plane (2013), A global atmospheric model of meteoric iron, *J. Geophys. Res.*, *118*, doi:10.1002/jgrd.50708.

Gardner, C. S., J. M. C. Plane, W. Pan, T. Vondrak, B. J. Murray, and X. Chu (2005), Seasonal variations of the Na and Fe layers at the South Pole and their implications for the chemistry and general circulation of the polar mesosphere, *J. Geophys. Res.*, *110*(D10), D10302, doi: 10.1029/2004JD005670.

Gardner, C. S., X. Chu, P. J. Espy, J. M. C. Plane, D. R. Marsh, and D. Janches (2011), Seasonal variations of the mesospheric Fe layer at

Rothera, Antarctica (67.5°S, 68.0°W), *J. Geophys. Res.*, *116*, D02304, doi: 10.1029/2010JD014655.

Höffner, J., and J. Lautenbach (2009), Daylight measurements of mesopause temperature and vertical wind with the mobile scanning iron Lidar, *Opt. Lett.*, *34*, 1351–1353.

Lübken, F.-J., and J. Höffner (2004), Experimental evidence for ice particle interaction with metal atoms at the high latitude summer mesopause region, *Geophys. Res. Lett.*, *31*, doi:10.1029/2004GL019586.

Lübken, F.-J., U. Berger and G. Baumgarten (2009), Stratospheric and solar cycle effects on long-term variability of mesospheric ice clouds, *J. Geophys. Res.*, *114*, D00I06, doi:doi:10.1029/2009JD012377.

Lübken, F.-J., J. Höffner, T. P. Viehl, B. Kaifler, and R. J. Morris (2011), First measurements of thermal tides in the summer mesopause region at Antarctic latitudes, *Geophys. Res. Lett.*, *38*, doi:10.1029/2011GL050045.

Lübken, F.-J. (2013), Turbulent scattering for radars: A summary, *J. Atmos. Solar-Terr. Phys.*, *107*, 1–7, doi:10.1016/j.jastp.2013.10.015.

Lübken, F.-J., J. Höffner, T. P. Viehl, B. Kaifler, and R. J. Morris (2014), Winter/summer mesopause temperature transition in 2011/2012 at Davis (68°S), *Geophys. Res. Lett.*, *41*, doi:10.1002/2014GL060777.

Morris, R. J., D. J. Murphy, I. M. Reid, D. A. Holdsworth, and R. A. Vincent (2004), First polar mesosphere summer echoes observed at Davis, Antarctica (68°S), *Geophys. Res. Lett.*, *31*(16), L16111, doi: 10.1029/2004GL020352.

Morris, R. J., J. Höffner, F.-J. Lübken, T. P. Viehl, B. Kaifler, and A. R. Klekociuk (2012), Experimental evidence of a stratospheric circulation influence on mesospheric temperatures and ice-particles during the 2010–2011 austral summer at 69°S, *J. Atmos. Solar-Terr. Phys.*, *89*, doi: 10.1016/j.jastp.2012.08.007.

Murray, B. J., and J. M. C. Plane (2005), Uptake of Fe, Na and K atoms on low-temperature ice: implications for metal atom scavenging in the vicinity of polar mesospheric clouds, *Phys. Chem. Chem. Phys.*, *7*, 3970–3979.

Plane, J. M. C. (2003), Atmospheric chemistry of meteoric metals, *Chem. Rev.*, *103*, 4963–4984, doi:10.1021/cr0205309.

Plane, J. M. C., B. J. Murray, X. Chu, and C. S. Gardner (2004), Removal of meteoric iron on polar mesospheric clouds, *Science*, *304*(5669), 426–428, doi:10.1126/science.1093236.

Plane, J. M. C. (2012), Cosmic dust in the earth's atmosphere, *Chem. Soc. Rev.*, *41*, 6507–6518.

Plane, J. M. C., W. Feng, E. M. C. Dawkins (2015), The Mesosphere and Metals: Chemistry and Changes, *Chem. Rev.*, doi:10.1021/cr500501m.

Raizada, S., M. Rapp, F.-J. Lübken, J. Höffner, M. Zecha, and J. M. C. Plane (2007), Effect of ice particles on the mesospheric potassium layer at spitsbergen (78° n), *J. Geophys. Res.*, *112*, D08307, doi:10.1029/2005JD006938.

Rapp, M., F.-J. Lübken, A. Müllemann, G. Thomas, and E. Jensen (2002), Small scale temperature variations in the vicinity of NLC: Experimental and model results, *J. Geophys. Res.*, *107*(D19), 4392, doi: 10.1029/2001JD001241.

Rapp, M., and F.-J. Lübken (2004), Polar mesosphere summer echoes (PMSE): Review of observations and current understanding, *Atm. Chem. and Phys.*, *4*, 2601–2633.

Russell, J. M. III, S. M. Bailey, L. L. Gordley, D. W. Rusch, M. Horanyi, M. E. Hervig, G. E. Thomas, C. E. Randall, D. E. Siskind, M. H. Stevens, M. E. Summers, M. J. Taylor, C .R. Englert, P. J. Espy, W. E. McClintock, A. W. Merkel (2009), The Aeronomy of Ice in the Mesosphere (AIM) mission: Overview and early science results, *J. Atmos. Solar-Terr. Phys.*, *71*, 289–299, doi:10.1016/j.jastp.2008.08.011.

Self, D. E., and J. M. C. Plane (2003), A kinetic study of the reactions of iron oxides and hydroxides relevant to the chemistry of iron in the upper mesosphere, *Phys. Chem. Chem. Phys.*, *5*, doi:10.1039/b211900e.

She, C. Y., B. P. Williams, P. Hoffmann, R. Latteck, G. Baumgarten, J. D. Vance, J. Fiedler, P. Acott, D. C. Fritts and F.-J. Lübken (2006), Simultaneous observation of sodium atoms, NLC and PMSE in the summer mesopause region above ALOMAR, Norway (69°N, 12°E), *J. Atmos. Solar-Terr. Phys.*, *68*, 93–101, doi:10.1016/j.jastp.2005.08.014.

Thayer, J. P., and W. Pan (2006), Lidar observations of sodium density depletions in the presence of polar mesospheric clouds, *J. Atmos. Solar-Terr. Phys.*, *68*, 85–92, doi:10.1016/j.jastp.2005.08.012.

von Zahn, U., and J. Höffner (1996), Mesopause temperature profiling by potassium lidar, *Geophys. Res. Lett.*, *23*, 141–144.

Yu, Zh., X. Chu, W. Huang, W. Fong, and B. R. Roberts (2012), Seasonal variations of the Fe layer in the mesosphere and lower thermosphere: Four season variability and solar effects on the layer bottomside at McMurdo (77.8°S, 166.7°E), Antarctica, *J. Geophys. Res.*, *117*, D22302, doi: 10.1029/2012JD018079.